Research Article Open Access

E. G. Bortchagovsky*

Simple modeling of the ratio of fields at a tip and at contacting surface

DOI 10.1515/nansp-2016-0002
Received December 1, 2015; accepted February 24, 2016

Abstract: The proposed concept of Raman probe for near-field optical microscopy raises the question about the similarity of fields acting on specimens deposited at the tip apex and contacting surface. The signal generated at these two close but different points is defined by local fields, so it is the ratio of the fields at these points, that is the quantity of interest here. This work is concerned with the application of a simple dipole model for the analysis of the ratio of fields at the tip apex and at contacting surface as a function of their separation.

Keywords: dipole interaction, image dipole, scanning near-field optical microscopy, tip-enhanced Raman scattering, Raman probe, field enhancement.

1 Introduction

The concept of Raman probe for scanning near-field optical microscopy was proposed in 2012 by Bortchagovsky and Fischer [1]. This probe is a functionalized tip covered by a Raman active material and it is the signal of Raman scattering collected from this material, which gives the information about local environment or local field distribution at the probe. Considering the sensitivity of Raman spectra to the variety of physical and chemical interactions such a probe transduces different interactions to the optical signal [1]. This approach likes Kopelman ideas of the use of his excitonic tip [2,3] as different fluorescing sensors, which are reviewed in [4].

Raman probes can also monitor the distribution of the local field as it was made with a tip functionalized by a nanocrystal with fluorescent centers [5]. In contrary to the use of fluorescence [2,3,5], Raman probe can use nonresonant Raman scattering and needs only monolayer coverage to function. So this Raman probe does not suffer from bleaching and its resolution is the same if the tip had not been functionalized. Raman probes were proposed as an internal standard in tip-enhanced Raman scattering (TERS) [6]. Considering the nonlinear dependence of the Raman signal versus the field intensity such an application is inherently approved. However this and similar applications beg the questions: what is the relation of fields at the tip apex and contacting surface and would it allow comparison of signals from materials at these two points. In spite of very close proximity of those two points, asymmetry of the structure due to very different shape of the tip and surface results in different field distribution and nonequivalent positions for coverage at these two parts. In this work, we analyze of the relation of fields at those two points using a simple model.

2 Relation of fields at the tip and at contacted flat surface

Formally, there is no principal difference between TERS configurations when the Raman active substance is deposited on a substrate and on a tip. If the scanning is performed in constant gap mode, the fields and the enhancements at the surface and at the tip are close and often considered as equal. This is true for the following reasons:

The positions at the tip and at the surface coalescence upon contact, so formally the fields at the tip and at the surface are equal in this case. At small separation for usual scanning conditions the difference of these fields can not drastically increase. To show this, consider an infinite flat capacitor, which is well known to have constant interior field (Fig.1a). If the capacitor is then restricted to have finite size as in Fig.1b, the disturbance of the field at the edges penetrates the capacitor and the nonuniformity of the field in the middle rises with the separation of plates (d) and decreases with increasing of the size of the capacitor (L). In the case of the tip in front of the surface

***Corresponding author E. G. Bortchagovsky,** Institute of Semiconductor Physics of NASU, pr. Nauki 41, 03028 Kiev, Ukraine, E-mail: bortch@yahoo.com

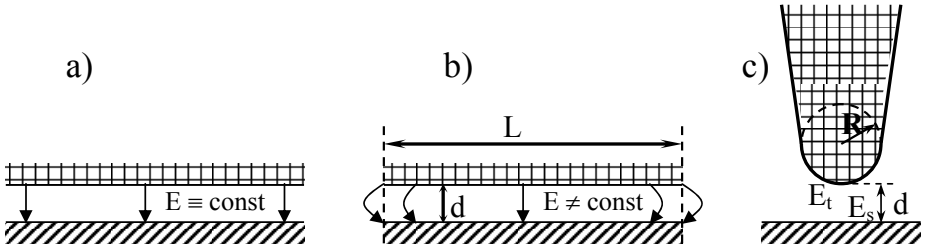

Fig.1. Infinite flat capacitor (a), finite flat capacitor (b) and the situation of scanning in TERS (c).

(Fig.1c) one plate of this capacitor is "infinite" plane as the second one is restricted in size curved "plate". The "width" of the curved plate is determined by the radius of the curvature of the apex (R), and plays the role of the size of our capacitor, as the gap width at scanning (d) is the separation of plates.

Our task is to determine the behavior of the ratio of fields at the tip (E_t) and at the surface (E_s). As this ratio is dimensionless, it can be determined only by other dimensionless quantities. In our case we have two linear values – the gap width (d) and the apex curvature (R), so the only dimensionless combination is their ratio. It is obvious when one considers capacitors that just d/R should be used, since either d=0 or R→ ∞ is the trivial case where $E_t/E_s = 1$. However if the radius of the apex curvature decreases to tens of nanometers in the best real case, the gap width is usually only few nanometers with AFM feedback and about 1nm with STM feedback. So the parameter d/R is small and any function describing the behavior of the ratio of fields E_t/E_s as a function of d/R can be expanded in a series according to this small parameter. Thus, no matter how complex is the real model which describes the value of fields at the tip and at the surface, the ratio of these fields is close to unity and depends almost linearly on the ratio d/R at small separations.

For the approximation of the coefficients of that series let us consider the simple model of a polarizable sphere over a flat surface to mimic the field distribution in the gap between the tip and the substrate (Fig.2a). Despite of the simplicity of this model, it is used as a toy example in many studies giving qualitatively and sometimes quantitatively correct results [7,8].

If the tip is close to the surface what happens at scanning, we can use the Rayleigh approximation keeping only the strongest term in the expression of the dipole field, which in this case is inversely proportional to the cube of the distance. Standard expression for the polarizability of a sphere in ambient is [9,10]

$$\alpha = r_t^3 \frac{\varepsilon_t - \varepsilon_a}{\varepsilon_t + 2\varepsilon_a} \tag{1}$$

where r_t is the radius of the sphere and ε_t and ε_a are dielectric functions of the sphere material and the ambient correspondingly. This sphere is polarized by the illuminating field and we distinguish between two cases for the generated dipole moment along and across the surface, shown in Fig. 2b-c.

The dipole generated on the sphere is situated at the center of the sphere, i.e. on the distance $z=(r_t+d)$ from the surface. This dipole polarizes the substrate, which in turn generates additional polarization of the sphere. The additional field produced by the substrate polarization can be described in the Rayleigh approximation as the field of an image dipole situated at a depth z under the surface, which has amplitude [9,10]

$$P_{im} = KP \tag{2}$$

where P is the amplitude of the sphere dipole, $K = \frac{\varepsilon_s - \varepsilon_a}{\varepsilon_s + \varepsilon_a}$ and ε_s is the dielectric function of the substrate. In the case of a free sphere, its dipole moment is defined by the expression $P=\alpha E_0$, and in the case of a sphere at the surface it is given by the expression

$$P = \alpha (E_0 + E_{im}) \tag{3}$$

where E_0 is the external excitation field and E_{im} is the field generated by the surface polarization respectively.

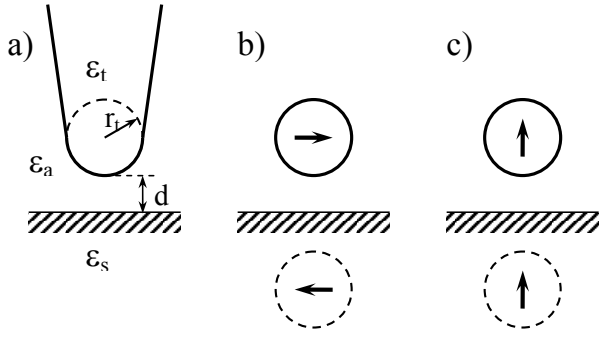

Fig.2. The model used for the analysis of fields behavior in TERS experiments.

The latter one over the surface is the dipole field, whose direction at the center of the sphere coincides with the direction of the illuminating field in both polarizations. Keeping only the strongest term in the expression for the value of this field we obtain in the case of the polarization along the surface $E_{im}=P_{im}/8z^3$. In the case of the polarization across the surface this value is twice as large [9,10]. All of these expressions produce self-consistent system. Substituting these values together with (2) into (3), we can easily solve this system to obtain the effective polarizability of the sphere renormalized by the close proximity of the substrate

$$\alpha' = \frac{\alpha}{1-\frac{\nu\alpha}{8z^3}\frac{\varepsilon_s-\varepsilon_a}{\varepsilon_s+\varepsilon_a}} \tag{4}$$

where ν is equal 1 or 2 for the case of the polarization along or across the surface. This renormalized polarizability can be used to calculate the dipole moment of the sphere at the substrate by the expression $P=\alpha' E_0$, and the image dipole can be calculated using (2). The field in the semispace, which comprises the sphere, is defined by these two dipoles [9,10], so we can obtain the field both at the tip apex and at the surface under the tip. Now the field's direction generated at those points by two dipoles coincide for the case of the transverse polarization across the surface but are opposite for the case of the longitudinal polarization along the surface. This observation agrees with known fact that the TERS signal is much stronger at the polarization across the surface. In this case we obtain

$$E_s = \frac{2\alpha' E_0}{z^3}(1+K), \qquad E_t = \frac{2\alpha' E_0}{z^3}\left(\left(\frac{r_t+d}{r_t}\right)^3 + \left(\frac{r_t+d}{r_t+2d}\right)^3 K\right) \tag{5}$$

The ratio E_t/E_s is a rather cumbersome expression but in the limit $d<<r_t$, what is the case especially with STM feedback we can obtain

$$\frac{E_t}{E_s} = 1+3\frac{d}{r_t}\frac{\varepsilon_a}{\varepsilon_s} \tag{6}$$

As mentioned, the deviation of the ratio of fields at the tip and at the surface from unity is defined by the ratio of the tip-surface separation to the radius of the curvature of the tip, since it is the smallness of this ratio, which approaches the real tip-surface geometry to the geometry of a flat capacitor with the constant field in the gap.

Note that if the fields at the tip and at the surface depend on the dielectric function of the material of the tip as it defines the amplitude of the generated dipole, the ratio of those fields does not depend on the tip material. This fact decreases the influence of unaccounted higher multipoles whose values depend on the concrete tip shape and general geometry of the system according to the angle of incidence and the polarization of the incident light.

For completeness note that the considered model has few obstacles in the calculation of the intensity of fields itself. The point dipole approximation normally overestimates the self-action due to the image field, so Metiu [11] proposed some correction by adding the screening length in the substrate to the dipole-image distance. At the same time, the approximation of the image field by the mirror imaged dipole has own restrictions working in the first for ideal metals [12]. Taking into account the effect of multipoles would also change the absolute value, remarkably enhancing the gap effect [13].

And the last but not least is the possible ambiguity of the approximation of the tip shape. For instance, a prolate or even oblate spheroid can be used instead of spherical tip shape. The prolate spheroid model would enhance the field at the apex due to the lighting-rod effect that can be easily described by the introduction of depolarization factor into the expression (1) [9,10]. At the same time the prolate shape would decrease the self-action in the point-dipole approximation due to larger distance of this spheroid's center to the surface. The opposite would be observed for the oblate spheroid model. Moreover, changing the tip shape in the model would, via the depolarization factor, changes the spectral resonant position for the particle, drastically changing the field values in some spectral ranges. Different first-principle calculations give the shift of the resonance of elongated cones to IR, as the cone length increases [14]. However any change of the model should remain the linear behavior of the correction term according the ratio d/r_t changing only the coefficient at this term, since just this ratio determines the deviation of the system from a plane capacitor.

The expression (6) gives the background for the use of the signal of some Raman active material deposited on the tip as the reference for the calibration of the Raman signal from substances deposited on the surface. The ratio (6) does not depend on the intensity of the incident light what makes the ratio of the Raman signals generated at those two points insensitive to the fluctuations of the illumination intensity. Only fluctuations of the tip proximity change the ratio of two fields. However if the proximity to the surface is smaller than the tip radius, fields at the tip and at the surface are close and even the fluctuations of the proximity δd, which, we assume, are in turn smaller than the proximity d itself, would induce small variation of the ratio of fields at the tip and at the surface. Thus, we conclude that the local variation of the enhancement, the intensity fluctuations of the illumination, and other

uncontrollable factors would almost equally contribute to the signal from substances on the tip and on the surface keeping their ratio practically constant.

It is necessary to note very restricted range of validity of the linear approximation (6) for good metals. The dielectric function of such metals is large and, as a consequence, the coefficient of the first member of the series expansion for d/r_t is small. As the result, the second member of the series expansion, which has a similar value in this case, should be accounted for. For example in the case of gold surface as in our experiment [6] the ratio $\varepsilon_a/\varepsilon_s$ at the wavelength of He-Ne laser is about −0.1 [15]. However the reality is even more favorable in this case. Taking into account the next term in the series would give the corrected expression

$$\frac{E_t}{E_s} = 1 + 3\frac{d}{r_t}\frac{\varepsilon_a}{\varepsilon_s} + 3\frac{d^2}{r_t^2}\left(3 - 2\frac{\varepsilon_a}{\varepsilon_s}\right) \tag{7}$$

Similar to the linear approximation in (6) this expression also does not depend on the dielectric function of the tip material. So, the tings we inferred about the influence of multipoles hold here too. Further it will be demonstrated that one obtains no qualitative change in the dependencies when one takes into account additional multipoles. Equation (7) is parabolic in d with minimum at d=-$rt\frac{\varepsilon_a}{\varepsilon_s}$/(6-4$\frac{\varepsilon_a}{\varepsilon_s}$), which is about 0.45nm when one uses the gold dielectric function ε_s=–11.8+i1.287 [15] and when the tip has radius of curvature 30nm, which is close to the real value [6]. This estimated position is of the same order of magnitude as the position of the minimum in Fig.3 calculated for the same parameters from the completed model expressions for fields of two point dipoles (5). In fact, it is easy to obtain the position of the minimum directly from (5) by differentiation with respect to d, which gives

$$d_{\min} = r_t \frac{\sqrt[4]{K} - 1}{2} \tag{8}$$

This analysis allows one to understand the general trend in the behavior of the ratio of fields at the apex and at the substrate directly underneath of the tip. Since the minimum occurs near 1nm separation, what is just the order of the separation at tunneling contact, that makes the dependence of the ratio of the fields less sensitive to the distance fluctuations. If the Raman signal is proportional to the fourth power of the field strength, the variation of the tip-surface separation in the range 0-1.6 nm would result in this model in <1% variation of the relative Raman signal of species deposited on the substrate and on the tip. When only the linear term is used with the same parameters, there is about 3% difference in the variation of the relative Raman signal [6]. At the same time the variation of the absolute Raman signal in the presented model for the case of a silver tip with radius of curvature 30nm and dielectric function ε_s=-18.219+i0.53 [15] situated at a flat gold substrate is more than twice the value for the same separation range. Such a difference in the change of the field intensity and the ratio of intensities supports the use of the Raman probe as an internal standard.

The smaller field at the tip apex in comparison to the field at the surface at small tip-surface separation does not sound right at first blush. However it can be explained by the existence of the surface plasmon in metals what is the consequence of the negative value of the metal dielectric function [16] as the frequency decreases. This results in a larger value of the image dipole P_m than the value of the source P as it may be seen in (2). As a consequence, the contribution from the image dipole to the field at the tip apex decreases faster than at the surface in the beginning of their separation. However the distance of the source dipole to the tip apex is constant as it is the tip radius while the image dipole moves off the surface and the tip. So, the contributions to the field at the surface from both source and image dipoles decrease, while the contribution of the source dipole to the field at the tip apex keeps constant. This behavior changes the situation quickly as it is seen in Fig. 3. This consideration suggests that larger negative value of the substrate dielectric function results in less difference between values of the image and the source dipoles, and as the result this difference looses its influence faster with separation. This fact would shift the minimum position in Fig. 3 to the origin. At the same time decreasing the absolute value of the substrate dielectric function so that it approaches

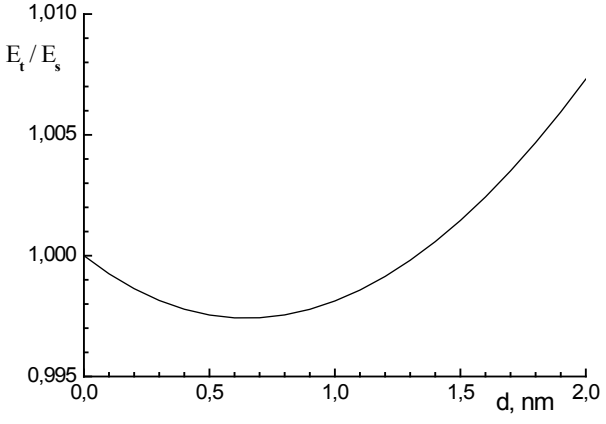

Fig.3. Dependence of the ratio of fields at the apex of a tip with the curvature of 30nm and at a flat gold surface versus the separation between the tip and the surface.

the conditions of the surface plasmon excitation would result in larger image dipole strength and longer range of its influence on the ratio of fields. The latter will shift the minimum to larger separation, as it is seen in Fig.4. The same behavior is visible from the expression for the position of the minimum of the parabola (7). In this way the surface plasmon not only improves the situation with the registration of TERS signal [17] but also lessens the difference between the fields at the tip apex and at the contacting surface at small separation. Surely, if the substrate dielectric function is positive, no plasmon effects exist, the image dipole is always smaller than the source dipole and the field at the tip apex is always larger than at the surface with no minimum at positive separation, which is shown in Fig.4.

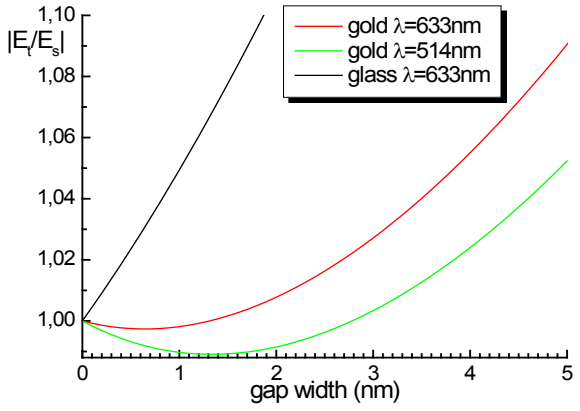

Fig.4. The ratio of fields at the apex of a tip with the curvature of 30nm and at flat surface is plotted against their separation for different choices of substrate material and wavelength.

Note that since the sphere in the model has finite size and is situated in the nonuniform field of the image dipole, its polarization is nonuniform too and the *center of mass* of the polarization is shifted from the center of the sphere to the substrate [13]. However omitted in the consideration the body of the tip, which is also polarized withdraws this *center of mass* back from the substrate. As the result this simple model reliably demonstrates the main features of the field distribution between the tip and the substrate.

This modeling shows that the introduction of the internal standard in TERS experiments by the deposition of a reference substance on the tip for the normalization of results by the Raman signal from the reference material [6] is robust. Presented calculations demonstrate that recorded signals are not only proportional but that the normalized result should be rather insensitive to feedback fluctuations. The same would be true for the fluorescence of both substances, provided one can avoid bleaching.

3 The case of a protrusion on the surface

A hemispherical protrusion of radius r_p can be treated in the context of the dipole model too, but now three image dipoles, and, in the case of transverse polarization, two opposite charges whose positions coincide with the positions of new dipole-images, are necessary as is shown in Fig.5 [10].

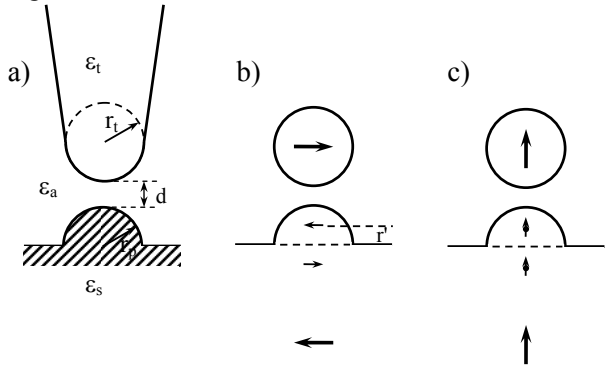

Fig.5. The case of a hemispherical protrusion on surface and position of all dipole-images.

Again the case having transverse polarization gives remarkable enhancement in comparison with the longitudinal one. Denoting

$$q = r_p/R\,, \quad r' = r_p^2/R = q\,r_p\,, \qquad P' = K\,q^3 P\,, \quad P_{im} = K\,P\,, \quad Q' = K\frac{r_p}{R^2}P \tag{9}$$

where R is the distance to the source, i.e. $R=r_t+d+r_p$ in our case, one can write the expressions for fields, which are bulky in this case [10]

$$E_s = \frac{2P}{(r_t+d)^3} + \frac{2P'}{(r_p-r')^3} + \frac{2P'}{(r_p+r')^3} + \frac{2P_{im}}{(r_t+d+2r_p)^3} + \frac{Q'}{(r_p-r')^3} - \frac{Q'}{(r_p+r')^3},$$
$$E_t = \frac{2P}{r_t^3} + \frac{2P'}{(r_p+d-r')^3} + \frac{2P'}{(r_p+d+r')^3} + \frac{2P_{im}}{(r_t+2r_p+2d)^3} + \frac{Q'}{(r_p+d-r')^3} - \frac{Q'}{(r_p+d+r')^3} \tag{10}$$

Using the relations

$$r_p - r' = q\,(r_t+d)\,, \quad r_p + r' = q(r_t+2r_p+d) \tag{11}$$

expressions (10) can be rewritten as

$$E_s = \frac{2\alpha' E_0}{z^3}\left((1+K) + \frac{2K(r_t+d)^3}{(r_t+2r_p+d)^3} + \frac{2K(r_t+d)(r_t+r_p+d)}{(r_t+2r_p+d)^2}\right),$$
$$E_t = \frac{2\alpha' E_0}{z^3}\left(\left(\frac{r_t+d}{r_t}\right)^3 + \left(\frac{q(r_t+d)}{q(r_t+d)+d}\right)^3 K + \frac{Kq^3(r_t+d)^3}{\left(q(r_t+2r_p+d)+d\right)^3} + \frac{K(r_t+d)^3}{(r_t+2r_p+2d)^3} + \frac{2Kq^3(r_t+d)^3(r_p+d)}{\left((r_p+d)^2-r'^2\right)^2}\right) \tag{12}$$

The ratio of these fields varies greatly with protrusion size. Small protrusions remarkably increase the magnitude of the field at the surface reflecting field enhancement near sharp features. This influence is shown in Fig.6.

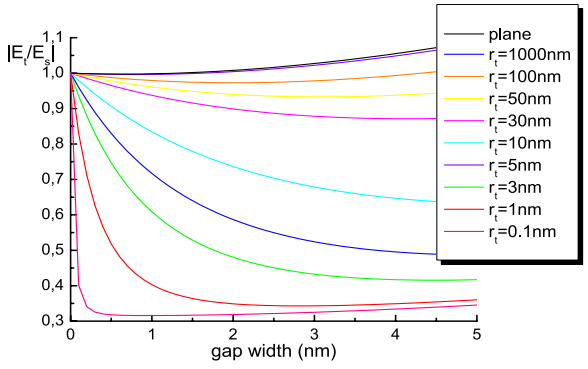

Fig.6. Dependence of the ratio of fields in (12) at the apex of a tip with curvature 30nm and at a protrusion on flat gold surface on their separation for different size of the protrusion.

It is interesting to note that as the result of the first relation in (11) the dipole-source at the tip and the closest dipole-image give at the protrusion surface the same field as it would have had the surface been flat, see Fig 7a. The small value of the image dipoles in the hemisphere is compensated for by its closure to the surface. The second relation in (11) results in the equal field from two remote images at the protrusion surface as shown in Fig.7b.
In the case of transverse polarization all fields are additive both at the surface and at the tip apex and additionally the fields at these points are increased by the imaged charges. However the contributions from these sources to the field at the tip are smaller since the distance is larger. It is especially pronounced for small protrusions when new imaged dipoles are very small (defined by q^3). The relation between fields from different images (11) demonstrated in Fig.7 explains the closeness to 1/3 of the minimum value of the curve for smallest protrusion size shown in Fig.6.

When one takes into account multipole effects, a large increase in the field strength is expected [13]. The influence of multipoles on the ratio of fields can be investigated in the further developed dipole model.

4 The influence of multipole effects

Since the sphere, which approximates the tip, has finite size and is situated in nonuniform fields of closely placed dipoles and charges, it has nonuniform polarization. This means that higher multipoles are generated on the sphere. These multipoles can be accounted for by the dipole model by considering images of external dipoles and charges in the sphere similar to those on the protrusion. In turn, those new sources generate new images in the surface and these compound effects ad infinitum [18], see the schematic in Fig.8.

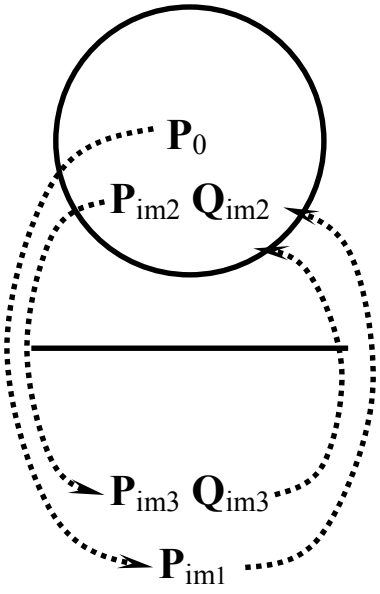

Fig.8. Schematic illustration of the sequential imaging of dipoles and charges in the system.

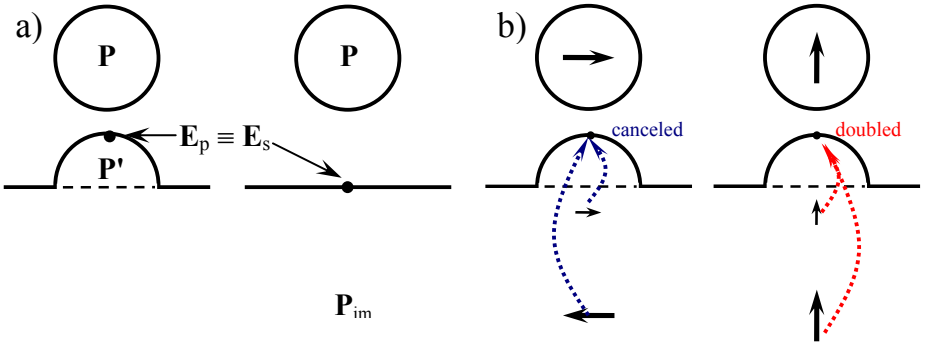

Fig.7. Fields from two dipoles at surface and relations between them.

The summation of infinite sequence of images is possible only when the sphere is situated directly on the surface [18]. The analytical solution when the sphere and surface do not touch is not tractable. However one can demonstrate the general influence of multipoles by approximating the solution using only the first few images. Fig.3 corrected by including the influence of the two next images is shown in Fig.9.

Since the sphere approximates a long tip with unknown shape, there is no sense to continue calculations with more and more images, but the overall behavior of the system is clear. Additional sources in the tip produced by the first image (see Fig.8) increase the field a great deal at the tip apex, but the addition of the next images returns the situation closer to the initial one. Only the minimum of the curve is a bit narrower and closer to the origin.

In the case of protrusion, the number of first imaged dipoles and charges is large. Consider the most interesting case of small protrusion, and for simplicity, let both dipoles be imaged in the protrusion at its center. The two opposite charges are combined into one more dipole. As the result, the dipole in the center will be 4 times larger than *P'*. In Fig.10 both the results shown in Fig.6 and this approximation as well as the account of the next image in the sphere for the latter case are shown.

The approximation works well but gives a bit bigger ratio. It is clear that the shift of all images in the protrusion into its center decreases the field at the surface, as the small closest image withdraws. Its field decreases proportionally to $1/r^3$ and the approach of the second, initially further separated, image-dipole does not compensate for this decrease. However the difference is not large and is almost compensated for by taking into account the next images in the tip. Considering the trend of the account of sequential imaging shown in Fig.9, we can expect something like oscillations of the ratio values between those curves.

5 Summary

The simple dipole model of the interaction of a tip and a substrate demonstrates features of the relationship of fields at the tip apex and at the contacting surface. It is shown that for flat surfaces this ratio is close to unity and varies only slightly with the separation between the tip and the surface. Moreover, when plasmon is present on the metallic surface, this decreases the variation resulting in an almost-constant field ratio over some distance. It makes the use of Raman probe as an internal standard in TERS [6] insensitive to the fluctuations of the feedback.

However the situation is different in the case of roughness. Used dipole model reproduces strong field enhancement at small protrusions on the surface. When the tip is drawn away from the surface, this results in sharp decrease in the ratio of fields and shows that it is necessary to account for details of the topography in the realization of the internal standard in TERS with the use of the Raman probe.

Note that only flat surfaces realize pure TERS measurements and avoid possible contribution from nonlocal SERS [19]. However, even on flat surfaces, it may be necessary to measure the variation of local enhancement, which exists on such substrates due to plasmonic interference [20].

The same model was used to take into account the influence of multipoles describing nonuniform

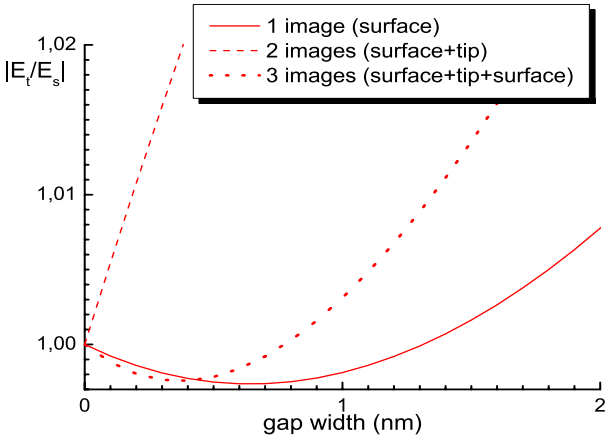

Fig.9. The ratio of fields at the apex of a tip with curvature 30nm and at the gold surface plotted against their separation, taking into account the first two sequential images.

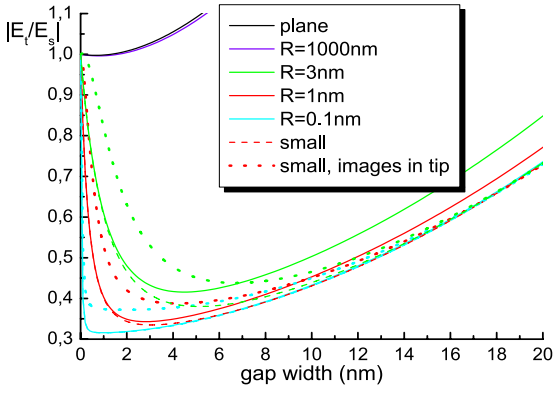

Fig.10. The ratio of fields at the apex of a tip with curvature 30nm and at a protrusion on gold plotted against their separation takeing into account the next few sequential images.

polarization of the tip, and their contribution to the ratio of the fields. Despite the large change in absolute values of fields after taking into account multipoles, there is only a small change in their ratio, which supports the robustness of the simple dipole model.

Acknowledgements: This work was performed in the context of the European COST Action MP1302 Nanospectroscopy.

References

[1] Bortchagovsky E., Fischer U., The concept of a near field Raman probe, Nanoscale, 2012, 4, 885-889.
[2] Lewis A., Kopelman R., A light source smaller than the optical wavelength, Science, 1990, 247, 59-61.
[3] Kopelman R., Lieberman K., Lewis A., Subwavelength molecular optics: the world's smallest light source?, Mol. Cryst. Liq. Cryst., 1990, 183, 333-340.
[4] Bortchagovsky E.G., Fischer U.C., Schmid T., Possibilities of functionalized probes in optical near-field microscopy, Phys. Scripta, 2014, T162, 014005-1-8.
[5] Aigouy L., Prieto P., Vitrey A., Anguita J., Cebollada A., Gonzalez M.U., Garcıa-Martın A., Labeguerie-Egea J., and Mortier M., Strong near-field optical localization on an array of gold nanodisks, J. Appl. Phys., 2011, 110, 044308-1-5.
[6] Bortchagovsky E., Schmid T., Zenobi R., Internal standard for tip-enhanced Raman spectroscopy, Appl. Phys. Lett., 2013, 103, 043111-1-3.
[7] Labani B., Girard C., Courjon D., van Labeke D., Optical interaction between a dielectric tip and a nanometric lattice: implications for near-field microscopy, J. Opt. Soc. Am. B, 1990, 7, 936-943.
[8] Keller O., Xiao M., Bozhevolnyi S., Configurational resonances in optical near-field microscopy: a rigorous point-dipole approach, Surf. Sci., 1993, 280, 217-230.
[9] Jackson J.D., *Classical electrodynamics, 3d ed.*, John Willey & Sons, New York, 1999.
[10] Sivukhin D.V., *The course of general physics, Vol.3, Electricity*, Nauka, Moscow, 1996 (in Russian).
[11] Metiu H., Surface enhanced spectroscopy, Prog. Surf. Sci., 1984, 17, 153-320.
[12] Lindell I.V., Alanen E., Exact image theory for the Sommerfeld half-space problem, Part II: Vertical electric dipole, IEEE Trans. Antennas Propagat., 1984, 32, 841-847.
[13] Jiang J., Bosnick K., Maillard M., Brus L., Single molecule Raman spectroscopy at the junctions of large Ag nanocrystals, J. Phys. Chem. B, 2003, 107, 9964-9974.
[14] Geshev P.I., Fischer U., Fuchs H., Calculation of tip enhanced Raman scattering caused by nanoparticle plasmons acting on a molecule placed near a metallic film, Phys. Rev. B, 2010, 81, 125441-1-16.
[15] Johnson P.B., Christy R.W., Optical constants of the noble metals, Phys. Rev. B, 1972, 6, 4370-4379.
[16] Raether H., *Surface plasmons on smooth and rough surfaces and on gratings*, Springer-Verlag, Heidelberg, 1986.
[17] Bortchagovsky E.G., Klein S., Fischer U.C., Surface plasmon mediated tip enhanced Raman scattering, Appl. Phys. Lett., 2009, 94, 063118-1-3.
[18] Bosi G., de Dormale B., Substrate-related effects on the optical behavior of granular surface: The Maxwell Garnett theory revisited, J. Appl. Phys., 1985, 58, 513-517.
[19] Deckert-Gaudig T., Deckert V., Ultraflat transparent gold nanoplates – ideal substrates for tip-enhanced Raman scattering experiments, Small, 2009, 5, 432-436.
[20] Maas H.-J., Naber A., Fuchs H., Fischer U.C., Weeber J.C., Dereux A., Imaging of photonic nanopatterns by scanning near-field optical microscopy, J. Opt. Soc. Am. B, 2002, 19, 1295-1300.